Search for diquark clustering in baryons

S. Fleck, B. Silvestre-Brac, and J. M. Richard
Institut des Sciences Nucléaires, 53 avenue des Martyrs, F-38046 Grenoble Cedex, France
(Received 22 March 1988)

In the framework of the nonrelativistic quark model, we examine to what extent baryons consist of a quark bound to a localized cluster of two quarks simulating a diquark. We consider ground states and orbital excitations for various flavor combinations. A striking clustering shows up sometimes especially for the leading Regge trajectory of the nucleon and single-flavored baryons or for the ground state of baryons bearing two heavy flavors. This is, however, far from being a general pattern and there are clear differences between the three-quark description of baryons and the quark-diquark model.

I. INTRODUCTION

Diquarks are almost as old as quarks. The notion of diquarks was already suggested by Gell-Mann in his pioneering papers on quarks,[1] and, since that time, there has been every year an abundance of literature on diquarks. The concept of diquark is, however, discussed from rather different points of view and some clarification is needed before presenting our contribution.

In some theories of fundamental structures, the diquark emerges from the very beginning as necessary for the internal consistency. This is the case, for instance, in the so-called topological bootstrap, see Nicolescu and Poenaru.[2] In such extreme approaches, the baryons are described as quark-antiquark bound states and the diquarks are either postulated as fundamental constituents on the same footing as quarks or built out of two quarks by *ad hoc* short-range forces.

In a more empirical approach, one does not postulate such new forces, but one assumes for simplicity that the baryon wave function consists of a quark orbiting around a set of two quarks whose clustering is due to the "ordinary" interquark potential only. For instance, in Ref. 3, the baryon binding energy is estimated in two steps: first by computing the mass of a cluster D out of two quarks and then by solving the two-body (D-q) problem. A good fit was obtained, but no comparison was attempted with the exact solution of the original three-body problem.

Our study is closer in spirit to the point of view adopted by Basdevant and Boukraa[4] and Martin.[5] In Ref. 4, a semirelativistic calculation of low-lying baryons was first done, using an extension of the hyperspherical formalism.[6] Then a comparison was shown with the two-step calculation, where the diquark D is built out of two quarks and the baryon computed as a q-D system, generally in rather good agreement with the three-body binding energy. In Ref. 5, a semiclassical calculation shows that with a two- or three-body linear confinement, associated with nonrelativistic or relativistic kinematics, the states of high angular momentum lying on the leading Regge trajectory consist of a quark well separated from the two others, which form a localized cluster. This explains why meson and baryon Regge trajectories have the same slope.

The aim of the present paper is to study systematically this dynamical clustering inside baryons. First, we compare the mass spectrum obtained from the whole three-body Hamiltonian to an approximate calculation where the baryon is made of a quark and a diquark. We also examine carefully the distribution of the interquark distances inside baryon wave functions obtained from an accurate three-body calculation. The nonrelativistic prototype presented here allows one to discuss the various factors which can act in favor of or against the formation of diquarks.

(i) Asymmetry of the system. In a (QQq) baryon with double charm or beauty, the two heavy quarks experience less kinetic energy than the light one, and tend to stay close to each other.

(ii) Angular momentum effect. One may be afraid that, if a baryon has a high spin, each pair of quarks should carry part of the angular momentum and, due to centrifugal repulsion, cannot form a diquark. The result of Ref. 5 suggests, however, that one quark takes care of the whole angular momentum whereas the two others form a diquark.

(iii) Spin effect. The quark-quark potential contains a spin-spin component which is short ranged and favors the formation of a diquark with spin 0.

(iv) Pauli principle. Such a spin-0 diquark is forbidden for identical quarks which should arrange themselves in a spin-triplet state for which the chromomagnetic forces are repulsive.

Each of these effects will be analyzed in detail. The asymmetry is studied by considering various flavor combinations $(q_1q_2q_3)=(qqq)$, (qqQ), or (qQQ) of light and heavy quarks, for which we examine all possible (q_iq_j) diquarks. In each case, the role of the angular momentum L is analyzed by considering states with $L=0$ and 8. Spin effects are exhibited by switching on and off the spin-dependent term of the potential. Comparing the (uuq) with the (udq) cases illustrates the constraints due to the Pauli principle.

The paper is organized as follows. The models and the relevant observables are defined in Sec. II. The nucleon system (qqq) is analyzed in detail in Sec. III, while the asymmetric configurations (qqQ) and (qQQ) are con-

sidered in Secs. IV and V. Our conclusions are drawn in the last section. Part of this work was already presented[7,8] and additional details will be provided elsewhere.[9]

II. THE MODELS

A. The potentials

We choose a simple constituent-quark picture of baryons, ignoring relativistic corrections, although they are certainly important for light quarks, especially to get a linear Regge behavior out of a linearly rising potential. Hopefully, the qualitative conclusions, concerning the presence or absence of clustering are not affected by the nonrelativistic approximation.

In the following, we shall adopt two different two-body potentials, which are representative of the various models commonly used in the literature. The first one is the familiar "Coulomb-plus-linear"[10] potential:

$$V_{ij}^{c}=\frac{1}{2}\left[-\frac{a}{r_{ij}}+br_{ij}+d\right], \tag{1}$$

which is supported by lattice calculations and which was extensively used for hadron spectroscopy.

The second one is the power-law potential

$$V_{ij}^{c}=\tfrac{1}{2}(A+Br_{ij}^{\beta}), \tag{2}$$

which has been proposed by Martin[11] for mesons and extended with some success to baryon spectroscopy.[12]

These potentials have to be supplemented by a hyperfine interaction of Breit-Fermi type:

$$V_{ij}^{ss}=\frac{C}{2}\frac{\boldsymbol{\sigma}_i\cdot\boldsymbol{\sigma}_j}{m_i m_j}\delta(\mathbf{r}_{ij}). \tag{3}$$

If one treats the spin interactions nonperturbatively, it is necessary to smear out the contact term (3), to avoid any collapse. One could use, for instance, the Yukawa form

$$V_{ij}^{ss}=\frac{C}{2}\frac{\boldsymbol{\sigma}_i\cdot\boldsymbol{\sigma}_j}{m_i m_j}\frac{e^{-\Lambda r_{ij}}}{r_{ij}}. \tag{4}$$

In the above formulas, m_i denotes the constituent-quark mass. The $\frac{1}{2}$ factor in front of the potentials is reminiscent from the rule $V_{qq}=\frac{1}{2}V_{q\bar{q}}$ which is often used to relate the quark potentials inside mesons and baryons.[12]

We use the potential corresponding to (1) + (4) as proposed by Bhaduri, Cohler, and Nogami[13] with the parameters

$a=0.5203$, $b=0.1857$ GeV^2 , $d=-0.9135$ GeV ,

$\Lambda=0.4341$ GeV , $C=0.0981$ GeV^2 ,

$m_q=0.337$ GeV , $m_s=0.600$ GeV ,

$m_c=1.870$ GeV , $m_b=5.259$ GeV .

A successful description of hadron spectroscopy has been achieved with this potential or with some improved versions elaborated by Ono and Schöberl[14] or others. A purely linear potential is of particular interest to study the leading Regge trajectory and test the semiclassical result of Martin.[5] We adopt in that case the linear part of the potential of Bhaduri, Cohler, and Nogami and force the rest of the potential to vanishing values. For the potential (2), we adopt the parameters of Ref. 12: namely,

$\beta=0.1$, $A=-8.337$ GeV , $B=6.9923$ GeV$^{1+\beta}$,

$m_q=0.300$ GeV , $m_s=0.600$ GeV ,

$m_c=1.895$ GeV , $m_b=5.255$ GeV .

In the investigations presented in the next sections, both potentials have been used with, in general, very similar results. This is why we will display only the density distributions corresponding to the Coulomb-plus-linear potential.

B. The quark-diquark approximation

For a given flavor configuration $(q_1q_2q_3)$, we assume *a priori* a diquark structure and approximate the exact three-body problem corresponding to the Hamiltonian

$$H=\sum_{i=1}^{3}\left[m_i+\frac{p_i^2}{2m_i}\right]+\sum_{i<j}V(r_{ij}) \tag{5}$$

by two successive two-body problems. First, a diquark is built out of the quarks q_2 and q_3, in s wave and color $\bar{3}$. If $q_2=q_3$, the diquark is forced to be in a spin $\sigma=1$ state as required by the Pauli principle, while nonidentical quarks give rise to a $\sigma=0$ diquark which is more favored energetically. More precisely, the diquark mass m_D is computed as the ground state of the two-body Hamiltonian:

$$H_{23}=m_2+m_3+\frac{p_2^2}{2m_2}+\frac{p_3^2}{2m_3}+V(r_{23}). \tag{6}$$

The diquark is now considered as a pointlike object and the approximate baryon mass is obtained from the Hamiltonian

$$H_{qD}=m_1+m_D+\frac{p_1^2}{2m_1}+\frac{p_D^2}{2m_D}+2V(r_{1D}). \tag{7}$$

The potential energy $2V(r_{1D})$ is deduced from $V(r_{12})+V(r_{13})$ in the limit $r_{12}=r_{13}=r_{1D}$. It is equal to the potential of a $q\bar{q}$ system. Spin-$\frac{1}{2}$ baryons are calculated in this approximation, with either angular momentum $L=0$ or $L>0$. In the latter case, the angular momentum is carried by the quark motion around the diquark. Similar calculations are also performed with the (q_2q_3) diquark replaced by (q_1q_2) or (q_1q_3).

Note that this approximation to the three-body problem might not be variational. Let us consider, indeed, the case of a harmonic-oscillator potential $V=\frac{3}{2}r^2$, with $m_1=m$ and $m_2=m_3=M$. Introducing the usual Jacobi coordinates $\boldsymbol{\rho}=\mathbf{r}_2-\mathbf{r}_3$ and $\boldsymbol{\lambda}=(\mathbf{r}_2+\mathbf{r}_3-2\mathbf{r}_1)/\sqrt{3}$ and the reduced mass μ given by $\mu^{-1}=\frac{1}{3}M^{-1}+\frac{2}{3}m^{-1}$, results in the Hamiltonian

$$H=\frac{p_\rho^2}{M}+\frac{p_\lambda^2}{\mu}+\rho^2+\lambda^2 , \tag{8}$$

whose lowest eigenenergy is $E_0=3M^{-1/2}+3\mu^{-1/2}$.

On the other hand, the quark-diquark approximation gives a diquark mass $m_D=2M+3\sqrt{2/3M}$, and a baryon energy $E_D=3\sqrt{2/3M}+3\tilde{\mu}^{-1/2}$, where $\tilde{\mu}^{-1}=\frac{2}{3}(m^{-1}+m_D^{-1})$. Clearly $E_D<E_0$. First, the reduced mass μ has been increased to $\tilde{\mu}$, resulting in a decrease of the kinetic energy. Also, the potential energy $\rho^2+\lambda^2$ has been decreased to $\frac{2}{3}\rho^2+\lambda^2$ by neglecting the diquark structure ($\mathbf{r}_{12}=\mathbf{r}_{13}=\mathbf{r}_{1D}$). Nothing can be said when the potential has negative powers as in the Coulomb case, or when spin forces are present.

C. Scrutinizing the wave function

The quark-diquark approximation of the previous section is tested only on its results for mass calculations, so even a good agreement with exact three-body energies would not prove that quarks do actually cluster. This is why we also calculate without approximation the three-quark wave function and look whether it contains any diquark structure. This calculation is achieved by expanding the three-body wave function $|\Psi\rangle$ on a harmonic-oscillator basis:

$$|\Psi_L\rangle=C\sum_{\sigma,n,l,m,k} d_{\sigma nlmk}\,|\chi_\sigma\rangle\,|[\phi_{nl}(\boldsymbol{\rho})\phi_{mk}(\boldsymbol{\lambda})]_L\rangle . \tag{9}$$

Here C denotes the color-singlet wave function, which is antisymmetric. For baryons with total spin $S=\frac{1}{2}$, there are two possibilities of spin coupling for the pair (2,3), $\sigma=0$ or 1, and thus, two basic spin functions $|\chi_\sigma\rangle=|\frac{1}{2}(\frac{1}{2},\frac{1}{2})_\sigma\rangle_{s=1/2}$. The spatial wave function is expanded on harmonic-oscillator basis $|\phi_{nl}\rangle$ for both relative Jacobi coordinates $\boldsymbol{\rho}$ and $\boldsymbol{\lambda}$ given by

$$\begin{aligned}\boldsymbol{\rho}&=\left[\frac{2m_2m_3}{m_2+m_3}\right]^{1/2}(\mathbf{r}_2-\mathbf{r}_3) ,\\ \boldsymbol{\lambda}&=\left[\frac{2m_1(m_2+m_3)}{m_1+m_2+m_3}\right]^{1/2}\left[\frac{m_2\mathbf{r}_2+m_3\mathbf{r}_3}{m_2+m_3}-\mathbf{r}_1\right] .\end{aligned} \tag{10}$$

The two oscillators are coupled to a total angular momentum L which is conserved here since tensor and spin-orbit forces are neglected. This way of solving the Schrödinger equation has been described elsewhere[15] in more detail. The total number of quanta $N=2n+l+2m+k$ is varied to check the convergence of the method. In practice, calculations performed in a basis with $N\leq 8$ turn out to be sufficiently accurate for our purpose. This means that we include 70 basis states for $L=0$ and 18 basis states for $L=8$. In the case of identical quarks, these numbers can be divided by two.

We define the one-body density $f_\sigma(\lambda)$:

$$\begin{aligned}f_\sigma(\lambda)&=\langle\Psi\,|\,P_\sigma\delta(\hat{\lambda}-\lambda)\,|\,\Psi\rangle\\ &=\int|\,P_\sigma\Psi(\boldsymbol{\rho};\boldsymbol{\lambda})\,|^2 d\boldsymbol{\rho}\,\lambda^2 d\Omega_\lambda\end{aligned} \tag{11}$$

with the normalization

$$\sum_\sigma\int_0^\infty f_\sigma(\lambda)d\lambda=1 . \tag{12}$$

Here P_σ is the projector that forces particles 2 and 3 to be coupled to a spin $\sigma=0$ or 1. Thus, the function $f_\sigma(\lambda)$ represents the probability density to find the particles 2 and 3 coupled to spin σ and particle 1 at a distance λ from the center of mass of the pair (2,3). We also define D as the value of λ which makes $\sum_\sigma f_\sigma(\lambda)$ maximum, i.e., the most probable distance between particle 1 and the pair (2,3).

We similarly define a two-body density $g_\sigma(\rho)$, by changing $\boldsymbol{\lambda}$ into $\boldsymbol{\rho}$ in the above formulas. The function $g_\sigma(\rho)$ represents the probability density to find particles 2 and 3 coupled to spin σ and at a distance ρ from each other. We call R the value of ρ which maximizes $\sum_\sigma g_\sigma(\rho)$, i.e., the most probable separation distance between quarks 2 and 3. If the density distributions $f_\sigma(\lambda)$ and $g_\sigma(\rho)$ are peaked such that $R\ll D$, this gives evidence for a (q_2q_3) diquark, as illustrated in Fig. 1(a). On the other hand, mean values such as $R\simeq D$ could reveal either the absence of diquark, as in Fig. 1(b) or a (q_1q_2) or (q_1q_3) clustering as in Fig. 1(c). To look for (q_1q_2) or (q_1q_3) clustering with the actual choice (10) of Jacobi coordinates, one should introduce the angular correlation between $\boldsymbol{\lambda}$ and $\boldsymbol{\rho}$ and define the three-body densities:

$$h_\sigma^{(\rho)}(\rho,\lambda,\theta)=\int|\,P_\sigma\Psi(\boldsymbol{\rho};\boldsymbol{\lambda})\,|^2\rho^2 d\Omega_\rho\lambda\sin\theta\,d\phi_{\rho\lambda} \tag{13}$$

normalized to

$$\int h_\sigma^{(\rho)}(\rho,\lambda,\theta)\lambda\,d\lambda\,d\theta=g_\sigma(\rho) \tag{13'}$$

and

$$h_\sigma^{(\lambda)}(\rho,\lambda,\theta)=\int|\,P_\sigma\Psi(\boldsymbol{\rho};\boldsymbol{\lambda})\,|^2\lambda^2 d\Omega_\lambda\rho\sin\theta\,d\phi_{\rho\lambda} \tag{14}$$

normalized to

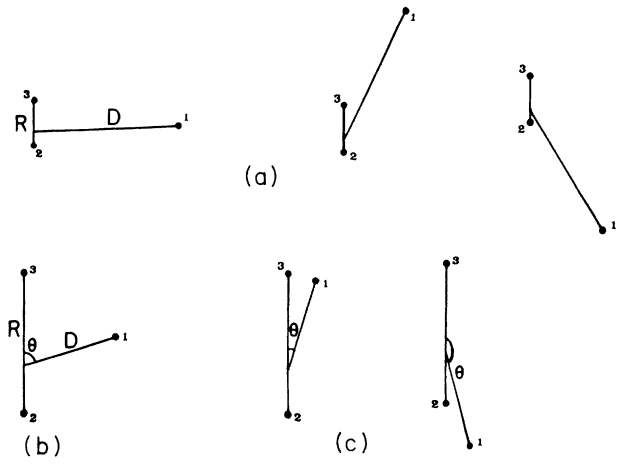

FIG. 1. Various geometries for quark distributions. R denotes the most probable interdistance between particles 2 and 3 while D is the most probable distance between particle 1 and the center of mass of the pair (2,3). Case (1.a), $R\ll D$. Case (1.b), $R\approx D$, $\theta=\pi/2$. Case (1.c), $R\approx D$, $\theta\approx 0$ or π.

$$\int h_\sigma^{(\lambda)}(\rho,\lambda,\theta)\rho\, d\rho\, d\theta = f_\sigma(\lambda) \tag{14'}$$

which are simply related by

$$\lambda h_\sigma^{(\rho)}(\rho,\lambda,\theta) = \rho h_\sigma^{(\lambda)}(\rho,\lambda,\theta)\ . \tag{15}$$

Here θ denotes the angle between $\boldsymbol{\lambda}$ and $\boldsymbol{\rho}$, and the integration measures have been chosen in order that $h_\sigma^{(\rho)}$ and $h_\sigma^{(\lambda)}$ are normalized as superficial densities with polar coordinates (ρ,θ) or (λ,θ). Up to some factors, the density h is the square wave function after some trivial azimuthal symmetries have been removed or integrated out. Slices of the distributions $h(\rho,\lambda,\theta)$ at fixed ρ or at fixed λ provide sets of planar densities which allow one for a systematic hunting of diquark clustering.

III. THE PROTON TRAJECTORY (duu)

A. The ground state $L=0$

We first analyze the case of the proton. The quark-diquark approximation described in Sec. II B is applied either for a vector diquark $(uu)_1$ or a scalar diquark $(ud)_0$. The comparison of the energies is presented in Table I. With central forces only, the diquarks $(uu)_1$ or $(ud)_0$ are identical, and for the various types of potentials considered here, the quark-diquark approximation is rather poor (15%), the approximate mass being lower than the exact one. When spin forces are included, the scalar diquark $(ud)_0$ is lighter and more closely clustered, but this does not improve the quark-diquark approximation. Let us remark that the Pauli principle is correctly taken into account for a $(uu)_1$ diquark, whereas, in the case of a $(ud)_0$ diquark, one neglects the antisymmetrization of the two u's inside the proton. Indeed, in the standard three-quark wave function of the proton, any (ud) pair is only $\frac{3}{4}$ of the time in a spin-singlet state.

We now examine the proton wave function, defined first as a d-(uu) configuration, for which the Jacobi variable $\boldsymbol{\rho} \propto \mathbf{r}_2 - \mathbf{r}_3$ is the distance between the two u quarks. The spin of the (uu) pair is $\sigma=1$. The density distributions $g_\sigma(\rho)$ and $f_\sigma(\lambda)$, shown in Fig. 2, reach their maxima at similar values $R=0.66$ fm and $D=0.50$ fm, respectively, so that no striking evidence for a (uu) diquark is seen. In the upper part of Fig. 3, we plot slices of the

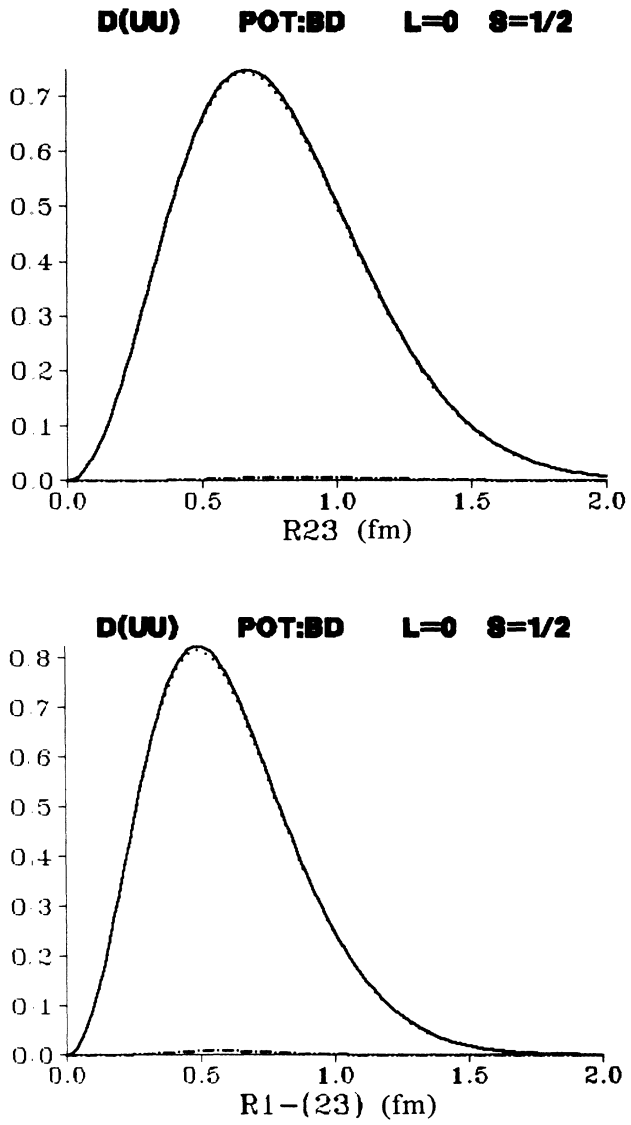

FIG. 2. Two-body density $g_\sigma(R_{23})$ (at the upper part) and one-body density $f_\sigma(R_{1\text{-}23})$ (at the lower part) plotted vs the corresponding physical distances (in fm) for the proton system in its ground state. The u and u quarks are coupled either to spin $\sigma=0$ (dotted-dashed line), to spin $\sigma=1$ (dotted line), or no matter the spin (solid line).

TABLE I. Total mass (in GeV) for the proton $(q_1q_2q_3)=(duu)$ system in its ground state obtained in a full three-body calculation (exact) and with an approximation based on two types of diquarks (q_2q_3) and (q_1q_2). Two central potentials [Martin (2) and Bhaduri, Cohler, and Nogami (1)] are tested and spin effects (4) are added in the potential of Bhaduri, Cohler, and Nogami. The mean-square radii (in GeV^{-1}) are given also.

Potential	$(\langle r_{23}^2\rangle)^{1/2}$	Exact $(\langle r_{12}^2\rangle)^{1/2}$	E_{exact}	Diquark $q_1(q_2q_3)$	Diquark $(q_1q_2)q_3$
Martin	5.078	5.078	1.086	0.907	0.907
Linear	4.725	4.725	2.818	2.634	2.635
Bhaduri central	4.439	4.333	1.204	1.023	1.024
Central $+\sigma\cdot\sigma$	4.348	4.032	1.032	0.740	0.912

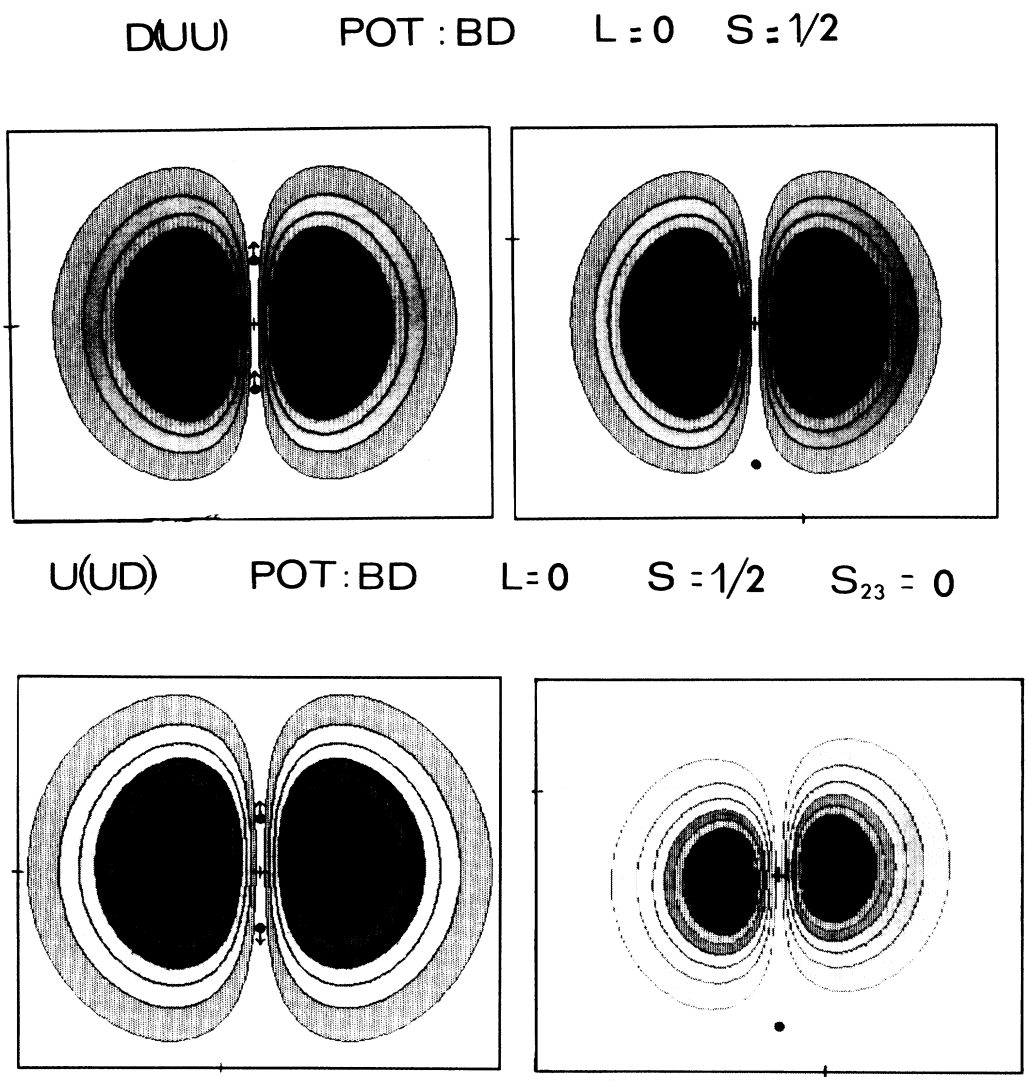

FIG. 3. Three-body densities $h_\sigma^{(\rho)}(R,\lambda,\theta)$ (left-hand part) and $h_\sigma^{(\lambda)}(\rho,D,\theta)$ (right-hand part) calculated for the proton system $L=0$ with the potential of Bhaduri, Cohler, and Nogami. In the upper part the particles 2 and 3 are the u quarks, while in the lower part, they are a u and a d quark. The cross at the center stands for the center of mass of the pair (2,3) and the scale measured from the bottom left corner is 1 fm. The "fixed" particles are symbolized by a black circle, and their spin coupling by arrows. The various grey slices represent the spatial probabilities of finding the remaining particles. The continuous lines separate regions with probabilities differing by 0.1, from the white outside (<0.1) to the extreme dark inside (>0.9).

three-body densities $h_1^{(\rho)}(R,\lambda,\theta)$ and $h_1^{(\lambda)}(\rho,D,\theta)$. In each case, one of the relative distance ρ and λ has been frozen to its most probable value. From this figure, there is no indication for a (ud) or (uu) type of diquark.

This conclusion is confirmed in a complementary analysis, where the proton is studied as a $u(du)$ configuration, with the Jacobi variable ρ attached to the d-u relative motion. As seen in the lower part of Fig. 3, where the $h_0^{(\rho)}(R,\lambda,\theta)$ and $h_0^{(\lambda)}(\rho,D,\theta)$ relative to a (ud) diquark coupling are plotted, all interquark distances have comparable mean values in the proton wave function resulting from our simple nonrelativistic model.

B. The $L=8$ excited state

The $d(uu)_1$ and $u(ud)_0$ quark-diquark approximations are now applied with the angular momentum $L=l_\lambda=8$ carried by the relative motion of the quark and the diquark. The results are presented in Table II for the linear and the potential of Bhaduri, Cohler, and Nogami. With central force only, the quark-diquark approximation is good up to 4%, being slightly better for the potential of Bhaduri, Cohler, and Nogami. When spin forces are added, the approximation remains good in both cases but the $d(uu)$ case seems better.

TABLE II. Same as in Table I for the proton (duu) system in an $L=8$ orbital excited state. Only linear and the potential of Bhaduri, Cohler, and Nogami are tested.

	E_{exact}	$q_1(q_2q_3)$	$(q_1q_2)q_3$
Linear	5.315	5.052	5.058
Bhaduri central	3.843	3.703	3.709
Central $+\sigma\cdot\sigma$	3.771	3.722	3.638

Let us now look at the wave function. The one-variable densities $g_\sigma(\rho)$ and $f_\sigma(\lambda)$ do not give much information in the $d(uu)_1$ channel, since $R=2.44$ fm and $D=1.36$ fm. As expected for an orbitally excited state, the system has a large spatial extension, but no diquark is seen so far. If we now turn to the $u(ud)$ configuration, the densities $g_\sigma(\rho)$ and $f_\sigma(\lambda)$ reach their maximum at $R=0.92$ fm and $D=2.28$ fm, respectively, indicating a (ud) diquark structure. This is confirmed clearly by the various extracts of the three-body density $h(\rho,\lambda,\theta)$ displayed in Fig. 4. This leads to two comments.

(i) Checking the validity of the quark-diquark approximation for the binding energy does not provide a very accurate test of the diquark structure. In the present example, it would favor $d(uu)_1$ against $u(ud)_0$.

(ii) Why is the $(ud)_0$ diquark favored in this specific calculation? There are, in fact, two conflicting effects. First, the $(ud)_0$ diquark is lighter than the $(uu)_1$, as a consequence of the chromomagnetic potential (3,4), and this favors the $(ud)_0$-u configuration with respect to $(uu)_1$-d. On the other hand, the $(uu)_1$-d binary system has a larger reduced mass and thus, experiences less kinetic energy when l is increased. In the present calculation, the first effect is still slightly dominant for $l=8$, but the state of $(ud)_0$-u structure is only 95 MeV below the $(uu)_1$-d one. As $l\to\infty$, the $(uu)_1$-d state would be the lowest one. In the real world, relativistic effects, spin-orbit forces, coupling to decay channels, etc., would greatly influence the ordering of these states.

IV. THE *Qqq* systems

We now study the influence of mass asymmetry by considering single-flavored Λ or Σ baryons with strangeness,

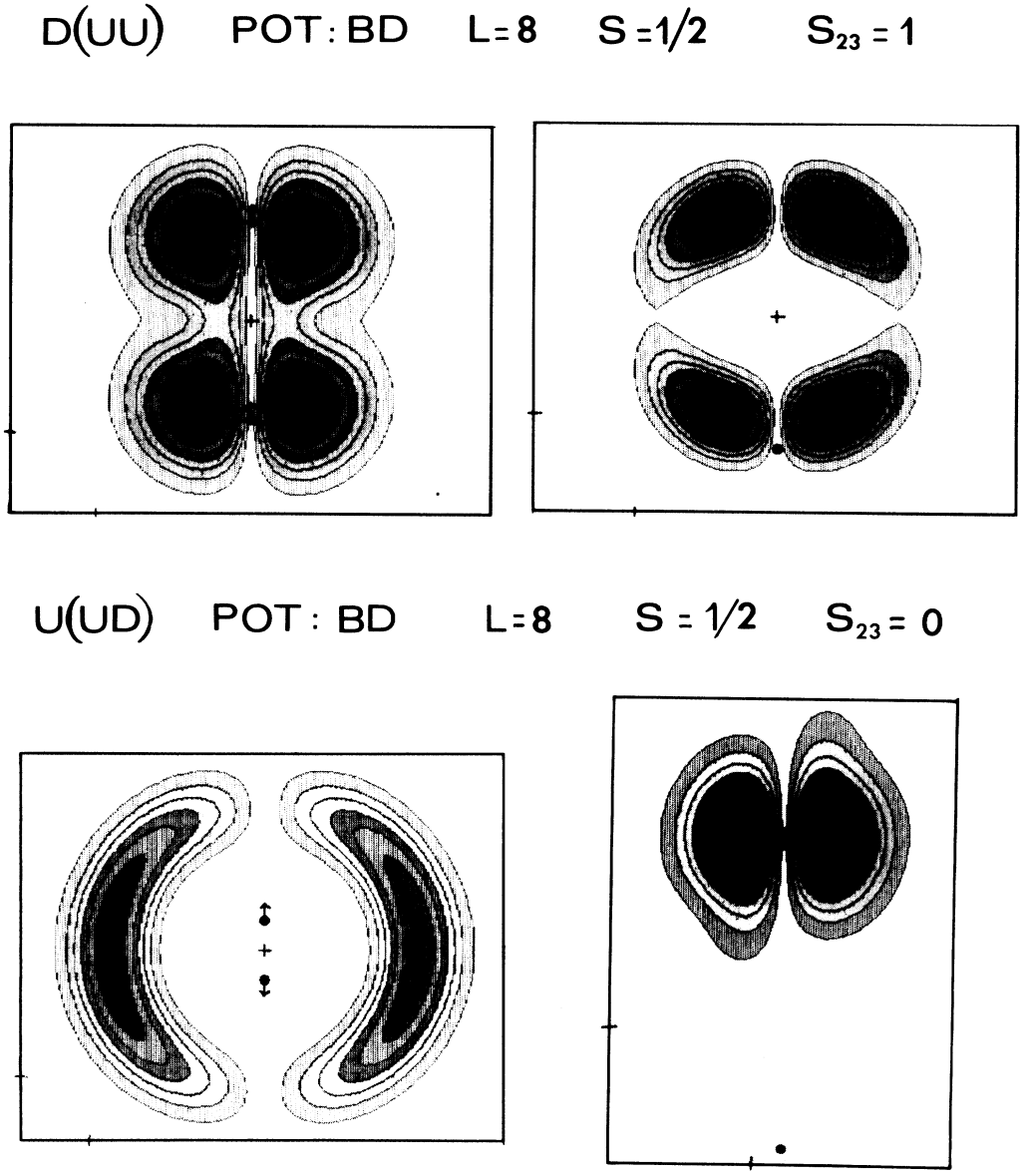

FIG. 4. Three-body densities for the proton system in an orbital $L=8$ excited state. Same comments as in Fig. 3.

TABLE III. Same as in Table I for two types of Qqq system: the $\Sigma = suu$ and the $\Sigma_c = cuu$.

Potential		Exact $(\langle r_{23}^2 \rangle)^{1/2}$	Exact $(\langle r_{12}^2 \rangle)^{1/2}$	E_{exact}	Diquark $q_1(q_2q_3)$	Diquark $(q_1q_2)q_3$
Martin	*suu*	4.934	4.481	1.268	1.321	1.234
	cuu	4.788	3.983	2.452	2.152	2.308
Linear	*suu*	4.688	4.362	2.983	2.772	2.835
	cuu	4.641	3.963	4.146	3.887	4.024
Bhaduri	*suu*	4.378	4.057	1.354	1.141	1.203
central	*cuu*	4.302	3.642	2.496	2.225	2.352
Central	*suu*	4.365	3.838	1.264	0.952	1.128
+	*sud*	3.859	3.863	1.186	1.037	1.129
spin-spin	*cuu*	4.391	3.608	2.493	2.155	2.323
	cud	3.440	3.790	2.327	2.136	2.324

charm, or beauty. As in the previous case, the $L = 0$ and 8 states are discussed separately.

A. The ground state $L = 0$

In Table III are displayed the results for the two possible diquark approximations Q-(qq) and (Qq)-q using various potentials. The Coulomb-plus-linear potential (1), the pure linear and the power-law (2) ones gives roughly the same conclusions. The quark-diquark approximations are antivariational, the Q-(qq) approximation corresponds to 10–15% deviation from the exact three-body energy while the (Qq)-q one is much better at around 4–6% deviation. So we note a clear correlation between the diquark radius and the accuracy of the quark-diquark approximation: as expected, the smaller (Qq) diquark gives a better result than the (qq) one.

When spin effects are included, the difference between the Q-(qq) and (Qq)-q approximations is enlarged and the latter is clearly favored. Also the Λ baryons are much

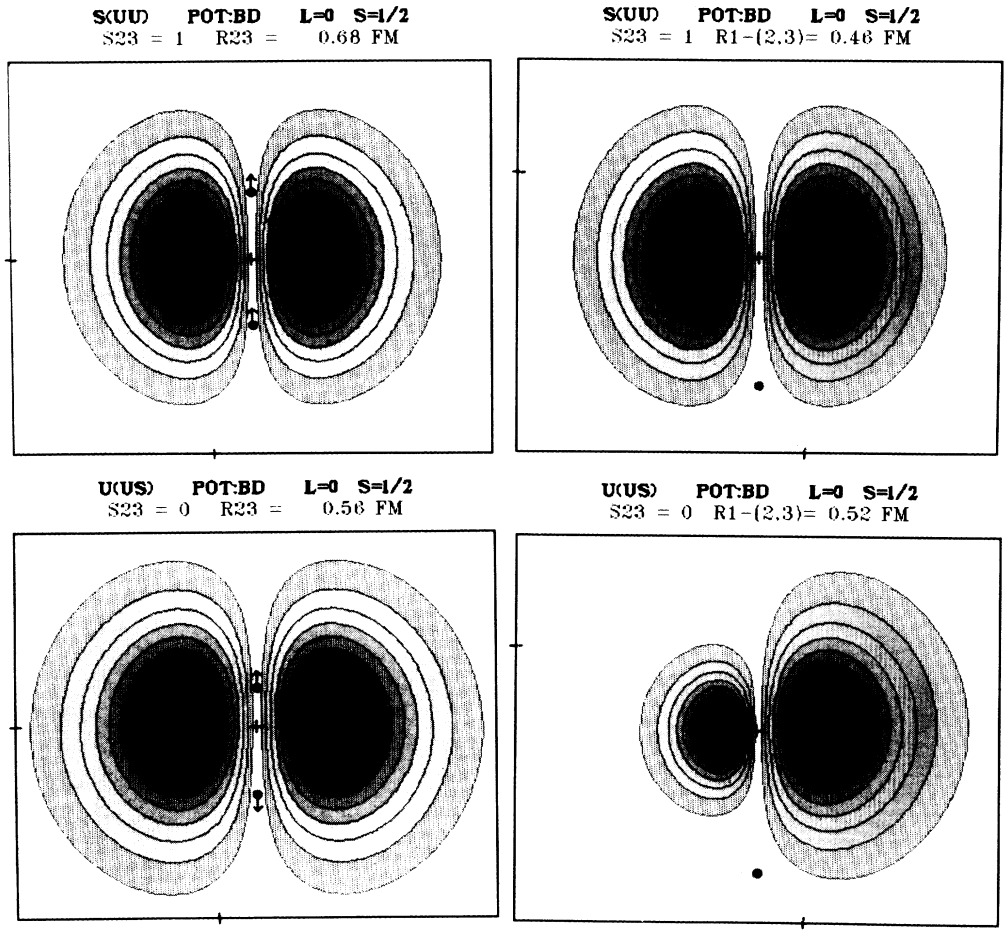

FIG. 5. Three-body densities for the Σ system suu in its ground state. Same comments as in Fig. 3.

better reproduced than the Σ one. In summary, the accuracy of the diquark approximation is around 12%, and cannot be considered as extremely good for the case of a (qq) diquark, while it is much better for the case of a (Qq) diquark.

The wave function of the $\Sigma(suu)$ is analyzed in Fig. 5, using either the u-u or the u-s distance as the Jacobi variable ρ. No diquark structure emerges. The size of the Σ is similar to the proton one, and the interquark distances have all the same average value of around 0.5 fm. No diquark structure was seen in other systems such as sdu, Quu, or Qud, where Q is some heavy quark.

B. The $L=8$ states

The quark-diquark approximation to the energy is shown in Table IV, for both Q-(qq) and (Qq)-q cases. We are in the embarassing situation where the approximations, although incompatible, seem both rather good (around 5%). In fact, the exact spectrum contains several nearly degenerate states, of Q-(qq) or of (Qq)-q type, each of those being approximated by a particular quark-diquark configuration.

We note a change with respect to the proton case, for which the (du)-u state was slightly below the (uu)-d one. Here the lowest state of the Σ type is found to be (uu)-s. The (us) diquark is obviously more deeply bound than the $(uu)_1$, but this is overcome by the fact that the $(uu)_1$-s system, having a larger reduced mass, acquires more easily orbital excitation than the $(us)_0$-u one. This tendency is even more pronounced for the cuu or buu cases. In Fig. 6 are shown the quark distribution densities for the

TABLE IV. Same as in Table III for the systems in an $L=8$ orbital excited state.

		E_{exact}	$q_1(q_2q_3)$	$(q_1q_2)q_3$
Linear	suu	5.213	4.868	5.235
	cuu	6.077	5.582	6.361
Bhaduri	suu	3.735	3.554	3.841
central	cuu	4.592	4.340	4.887
Central	suu	3.754	3.569	3.783
+	sud	3.667	3.502	3.785
spin-spin	cuu	4.609	4.348	4.859
	cud	4.531	4.318	4.862

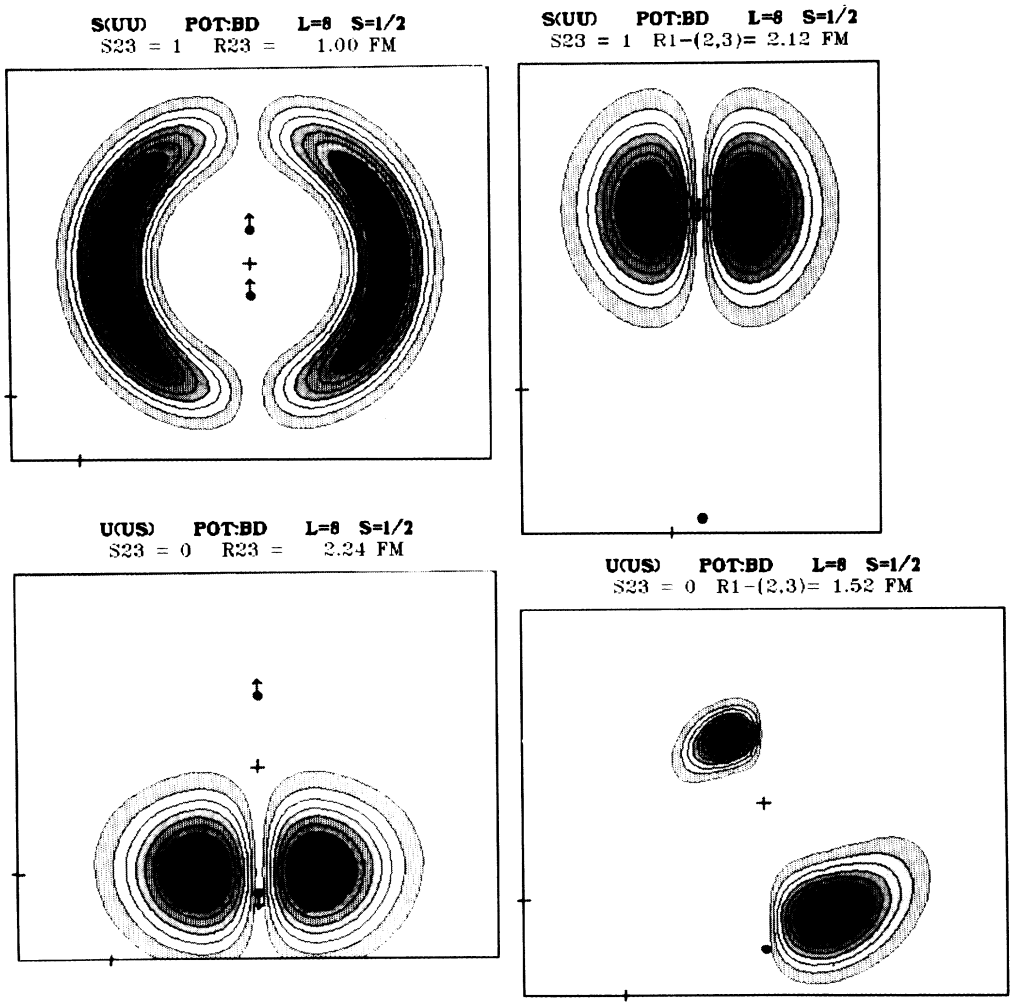

FIG. 6. Three-body densities for the Σ system suu in an orbital $L=8$ excited state. Same comments as in Fig. 3.

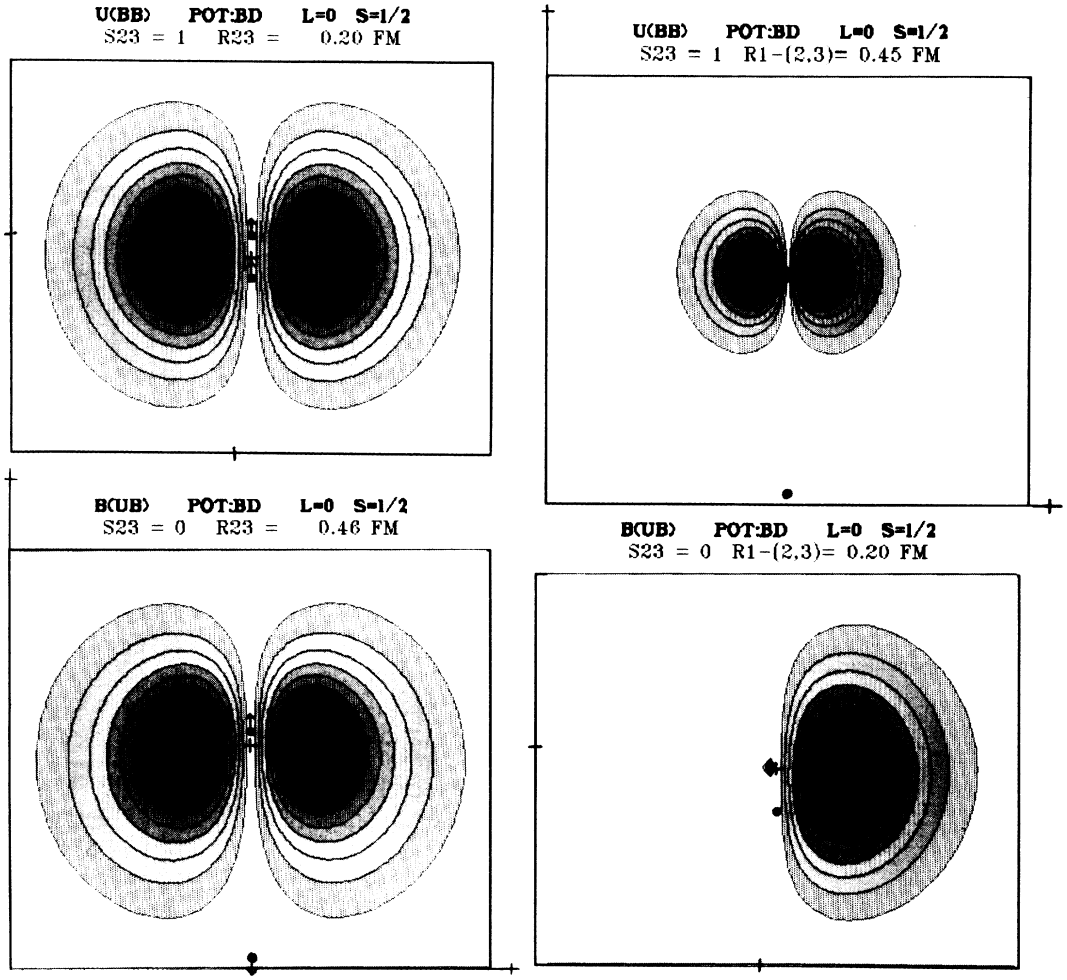

FIG. 7. Three-body densities for the *ubb* in its ground state. Same comments as in Fig. 3.

lowest Σ state. The four figures exhibit clearly a diquark structure of type (uu)-s.

V. THE qQQ SYSTEMS

A. The ground state $L=0$

In Table V, the various quark-diquark approximations are displayed. The quality of the results is the same for the different types of potential. Clearly, the (QQ) approximation is much closer than the (qQ) one to the exact result, and the bigger the ratio m_Q/m_q, the better the accuracy (7% for *uss*, 1% for *ucc*). When spin effects are added, the quality deteriorates but, if the masses are sufficiently heavy, the QQ diquark approximation gives again very good results.

The three systems *uss*, *ucc*, and *ubb* were studied in that case. When the mass ratio m_Q/m_q is not very large, there is no marked diquark structure; however when this ratio is increased, a QQ diquark structure becomes more and more apparent. We illustrate this point on the *ubb* system in Fig. 7. In at least two of the four figures, the QQ diquark is clearly signed. The natural tendency of the heavy particles to cluster each other is enforced by the attractive Coulomb part of the potential, whereas the repulsive spin effects are very weak, since they are proportional to m_Q^{-2}.

TABLE V. Same as in Table I for two types of qQQ system: the Ξ *uss* and the *ucc* systems.

Potential		Exact $(\langle r_{23}^2\rangle)^{1/2}$	Exact $(\langle r_{12}^2\rangle)^{1/2}$	Exact E_{exact}	Diquark $q_1(q_2q_3)$	Diquark $(q_1q_2)q_3$
Martin	*ucc*	2.326	3.673	3.685	3.634	3.396
	uss	3.782	4.338	1.430	1.321	1.234
Linear	*ucc*	2.756	3.847	5.409	5.357	5.237
	uss	3.937	4.322	3.141	3.025	2.969
Bhaduri	*ucc*	2.345	3.458	3.686	3.629	3.424
central	*uss*	3.612	3.995	1.493	1.375	1.311
Central	*ucc*	2.324	3.337	3.636	3.558	3.397
$+\sigma\cdot\sigma$	*uss*	3.543	3.711	1.373	1.173	1.239

B. The $L=8$ states

The corresponding results are presented in Table VI. The diquark approximation of type QQ does not work at all ($\sim 15\%$ accuracy) and always gives a mass larger than the exact one. On the other hand, the (qQ) diquark approximation is much better ($\sim 2\%$ accuracy) and is always antivariational.

The examination of the wave function is very interesting. We present here the *uss* system but the conclusions are essentially the same for *ucc*. Figure 8 corresponds neither to an isotropic configuration nor to a clear diquark structure. The state looks in fact like a QQ binary system, with a diluted q cloud in between. One can easily understand that one would never minimize the centrifugal energy $L(L+1)/\mu R^2$ with a (QQ)-q structure whose reduced mass is very light. The angular momentum is almost entirely carried by the relative motion of the two heavy quarks, i.e., $l_\rho=8$, whereas the light quark evolves in a s-wave state ($l_\lambda=0$), around the center-of-mass of two heavy quarks. One should probably need very high L to have a (Qq) diquark showing up.

C. The Born-Oppenheimer approximation for qQQ

We have just seen that, while a q-(QQ) quark-diquark approximation is acceptable for $L=0$, introducing angular momentum tends to separate the two heavy quarks without producing too much (qQ) clustering. In fact, the dynamics of the (qQQ) baryons is not well described in terms of diquarks. Instead, the Born-Oppenheimer method gives extremely convincing results.

TABLE VI. Same as in Table V for the systems in an $L=8$ orbital excited state.

		E_{exact}	$q_1(q_2q_3)$	$(q_1q_2)q_3$
Linear	*uss*	5.211	5.410	5.037
	ucc	6.854	7.667	6.745
Bhaduri	*uss*	3.728	3.985	3.669
central	*ucc*	5.340	6.129	5.285
Central	*uss*	3.694	3.997	3.618
$+\sigma\cdot\sigma$	*ucc*	5.326	6.132	5.260

For a fixed QQ separation ρ, one solves the one-body problem for the quark q, which is submitted to noncentral forces. Relativistic variants are even allowed, using, for instance, bag models. The binding energy $\epsilon_0(\rho)$ of the quark, when added to the direct QQ interaction $V_{23}(\rho)$, gives an effective two-body potential $\bar{V}_{QQ}(\rho)$, leading to a very accurate approximation of the first QQq energies and eigen-wave-functions. Higher states correspond to

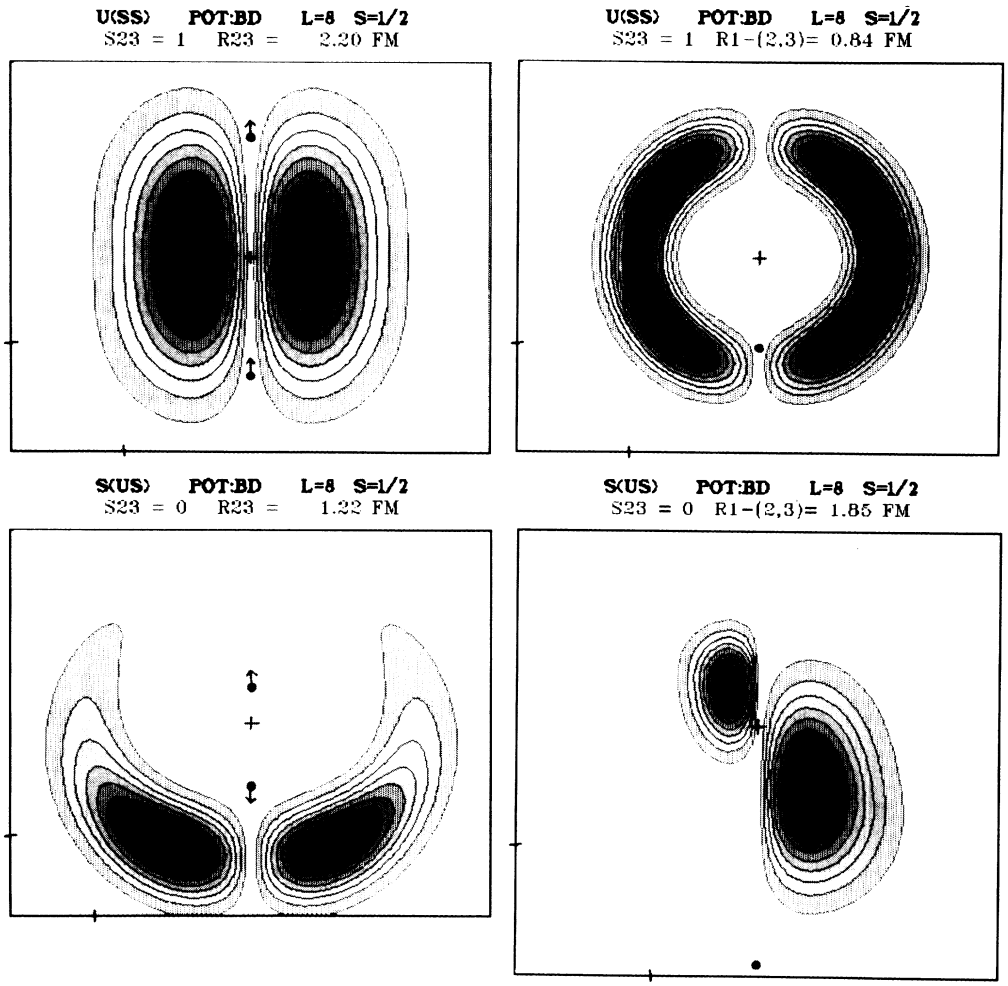

FIG. 8. Three-body densities for the Ξ system *uss* in an orbital $L=8$ excited state. Same comments as in Fig. 3.

second or higher adiabatics $\epsilon_n(\rho)$, $n>0$. As in many fields of physics, the Born-Oppenheimer method works much better than one would *a priori* expect. This is illustrated in Table VII. More details will be given elsewhere.[9]

TABLE VII. Comparison of the binding energies calculated exactly or in the Born-Oppenheimer approximation for the (ccu) system with the central potential (2).

	$L=0$	$L=1$	$(L=0)^*$
Born-Oppenheimer	3.6840	3.9689	4.1092
Exact	3.6848	3.9712	4.1096

VI. CONCLUSIONS

In this paper we have performed some nonrelativistic three-body calculations for various combinations of quark flavors, to examine to which extent baryons can be approximately described as a localized diquark surrounded by a quark. The comparison of the masses obtained in the quark-diquark approximation with the exact three-body calculation does not always provide unambiguous indications. Sometimes, a q_1-(q_2q_3) mass computed in the quark-diquark approximation coincides accidentally with the lowest $(q_1q_2q_3)$ system, whose structure is mostly (q_1q_2)-q_3.

Our conclusions concerning the diquark clustering in our simple nonrelativistic models are essentially based on a systematic study of quark correlations in the three-body wave function. There are only two cases where a diquark structure emerges clearly.

(i) In qQQ baryons with low angular momentum. The two Q quarks cluster under the combined effect of their heaviness, the attractive Coulomb potential, and the M_Q^{-2} suppression for the chromomagnetic repulsion.

(ii) In qqq or Qqq baryons with high angular momentum. In that case the centrifugal force which separates a single quark from a pair is the main ingredient. However, this type of diquark results from a subtle balance between the asymmetry which favors a qq diquark, and the spin-spin interaction allied to the Pauli principle, which favors a qQ diquark.

For $m_Q/m_q \gg 1$ a qq diquark will emerge, whereas for $m_Q/m_q \simeq 1$ a Qq diquark occurs.

For other systems, either the quark density is rather isotropic (low angular momentum qqq systems) or the resulting structure is of a molecular type (qQQ with high angular momentum). The arguments explaining diquark formation are "classical" in essence (for this we agree with Ref. 5); however, quantum effects cannot be ignored, especially the Pauli principle which forbids some configuration minimizing the classical Hamiltonian.

ACKNOWLEDGMENTS

We are particularly indebted to Professor C. Gignoux for many illuminating discussions and constant interest in this work. Advice and encouragement of A. Martin, P. Kroll, and E. Leader are gratefully acknowledged. We are very indebted to P. Olivero for valuable help concerning the graphical codes and to the Centre de Calcul de Physique Nucléaire for providing us computer facilities.

[1]M. Gell-Mann, Phys. Lett. **8**, 214 (1964).

[2]See, e.g., B. Nicolescu and V. Poenaru, in *A Passion for Physics*, proceedings of the G. F. Chew Jubilee, 1984, edited by C. DeTar, J. Finkelstein, and C.-I Tan (World Scientific, Singapore, 1985), pp. 195–221.

[3]D. B. Lichtenberg, W. Namgung, E. Predazzi, and J. G. Wills, Phys. Rev. Lett. **48**, 1653 (1982); K. F. Liu and C. W. Wong, Phys. Rev. D **28**, 170 (1983).

[4]J. L. Basdevant and S. Boukraa, Z. Phys. C **28**, 413 (1985).

[5]A. Martin, Z. Phys. C **32**, 359 (1985).

[6]M. Fabre de la Ripelle, in *Few Body System*, Suppl. 2 (Springer, Heidelberg, 1987), pp. 469–482 and 493–497.

[7]S. Fleck, B. Silvestre-Brac, C. Gignoux, and J. M. Richard, in *The Elementary Structure of Matter*, Les Houches, France, 1987, edited by J. M. Richard *et al.* (Springer, Heidelberg, 1988).

[8]B. Silvestre-Brac, Ann. Phys. Fr. **13**, 69 (1988).

[9]S. Fleck, thèse de l'Université de Grenoble I, 1988.

[10]See, e.g., W. Kwong, J. L. Rosner, and C. Quigg, Annu. Rev. Nucl. Part. Sci. **37**, 325 (1987).

[11]A. Martin, Phys. Lett. **100B**, 511 (1981).

[12]J. M. Richard and P. Taxil, Phys. Lett. **128B**, 453 (1983); Ann. Phys. (N.Y.) **150**, 267 (1983).

[13]R. K. Bhaduri, L. E. Cohler, and Y. Nogami, Nuovo Cimento **65A**, 376 (1981).

[14]S. Ono and F. Schöberl, Phys. Lett. B **188**, 419 (1982).

[15]B. Silvestre-Brac and C. Gignoux, Phys. Rev. D **32**, 743 (1985).

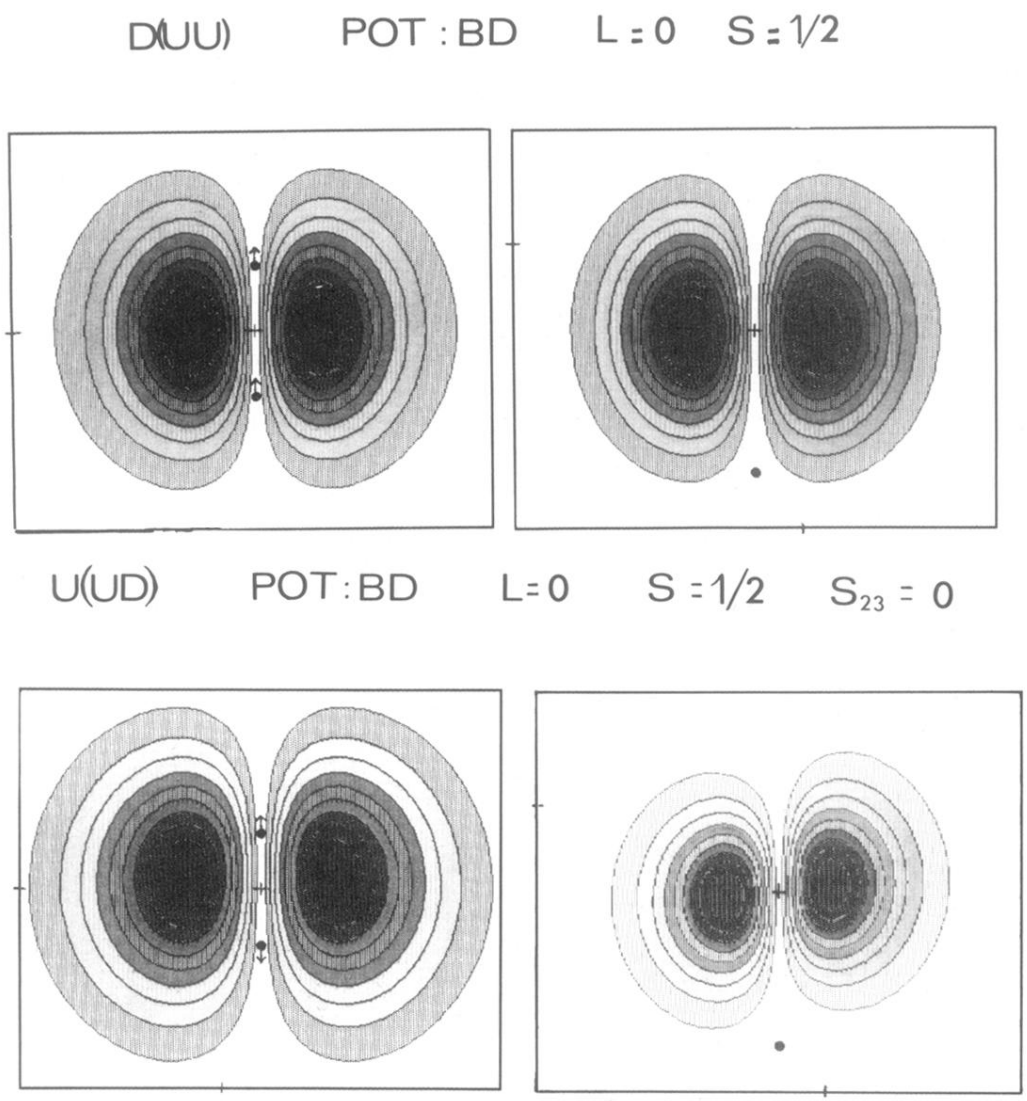

FIG. 3. Three-body densities $h_{\sigma}^{(\rho)}(R,\lambda,\theta)$ (left-hand part) and $h_{\sigma}^{(\lambda)}(\rho,D,\theta)$ (right-hand part) calculated for the proton system $L=0$ with the potential of Bhaduri, Cohler, and Nogami. In the upper part the particles 2 and 3 are the u quarks, while in the lower part, they are a u and a d quark. The cross at the center stands for the center of mass of the pair (2,3) and the scale measured from the bottom left corner is 1 fm. The "fixed" particles are symbolized by a black circle, and their spin coupling by arrows. The various grey slices represent the spatial probabilities of finding the remaining particles. The continuous lines separate regions with probabilities differing by 0.1, from the white outside (<0.1) to the extreme dark inside (>0.9).

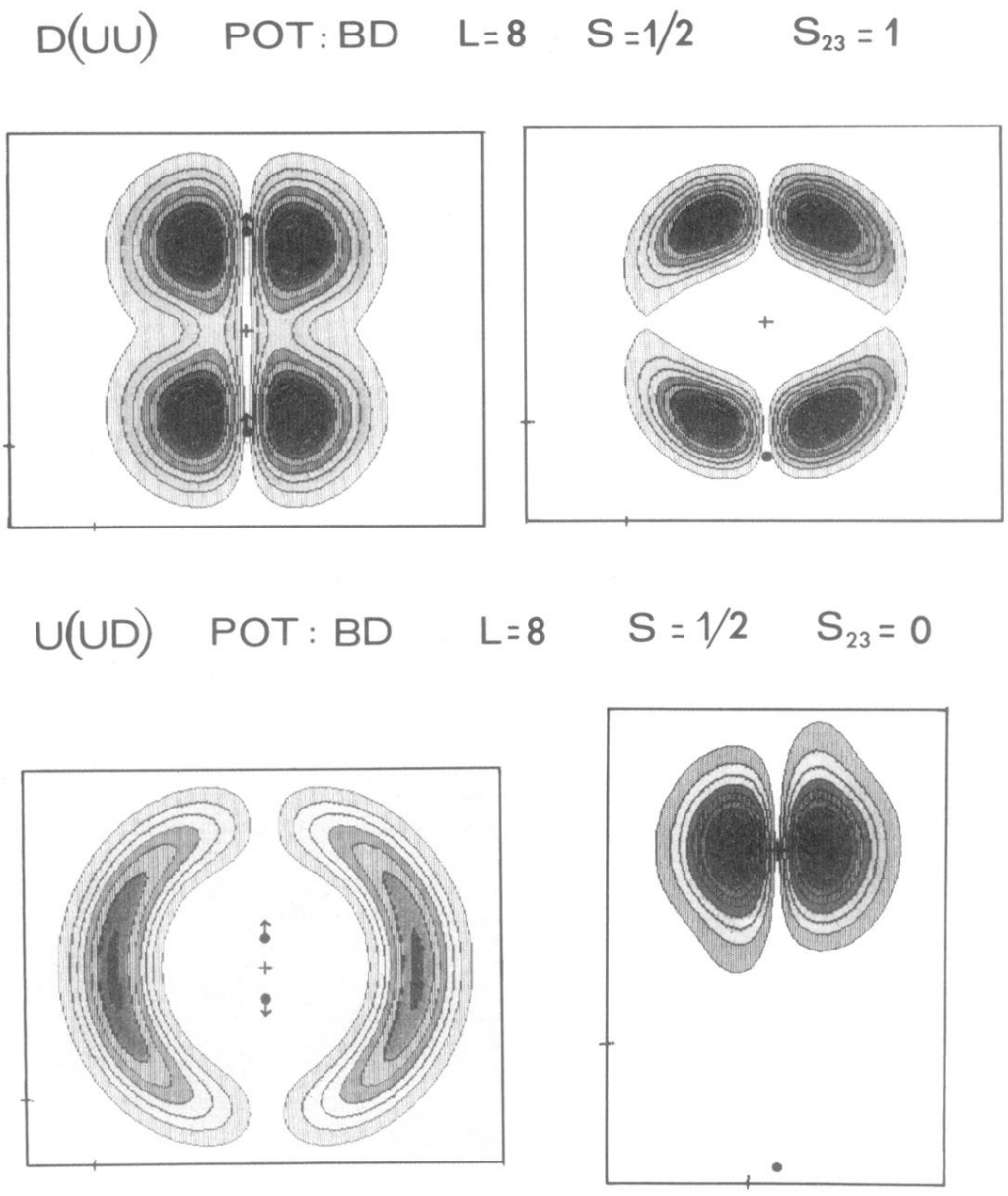

FIG. 4. Three-body densities for the proton system in an orbital $L = 8$ excited state. Same comments as in Fig. 3.

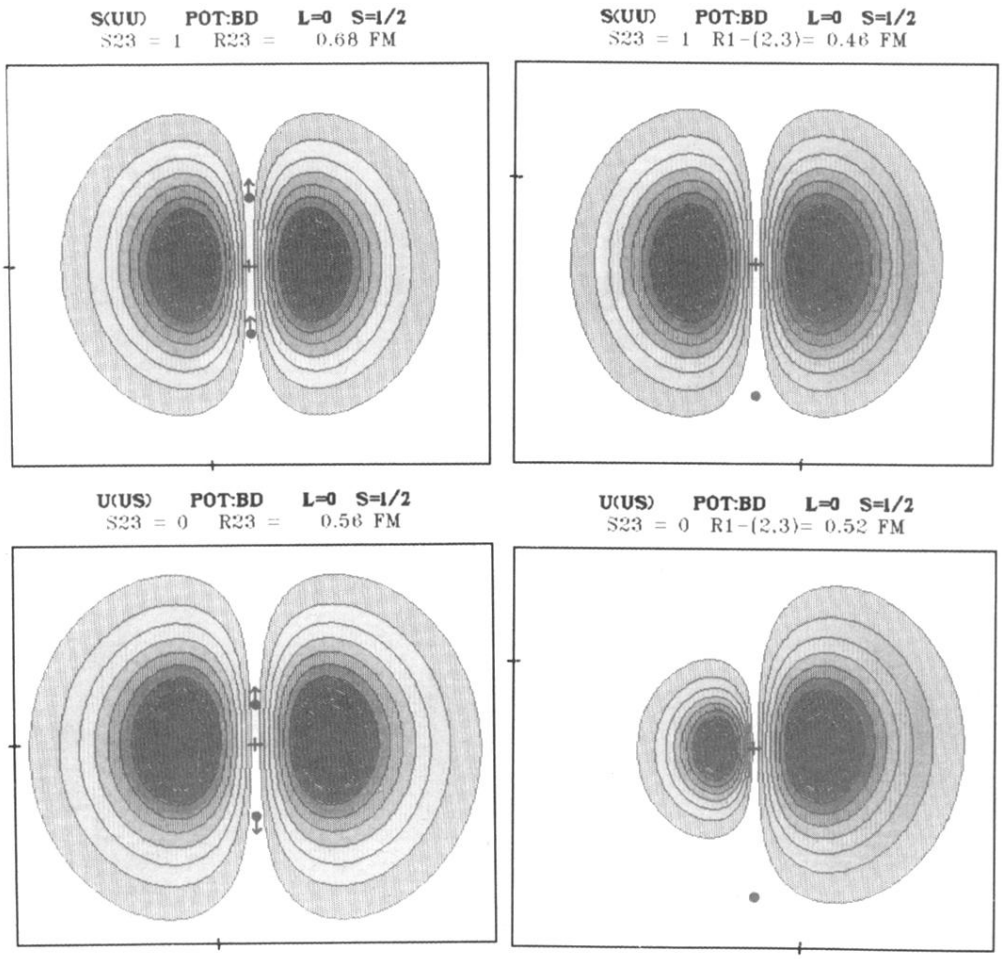

FIG. 5. Three-body densities for the Σ system *suu* in its ground state. Same comments as in Fig. 3.

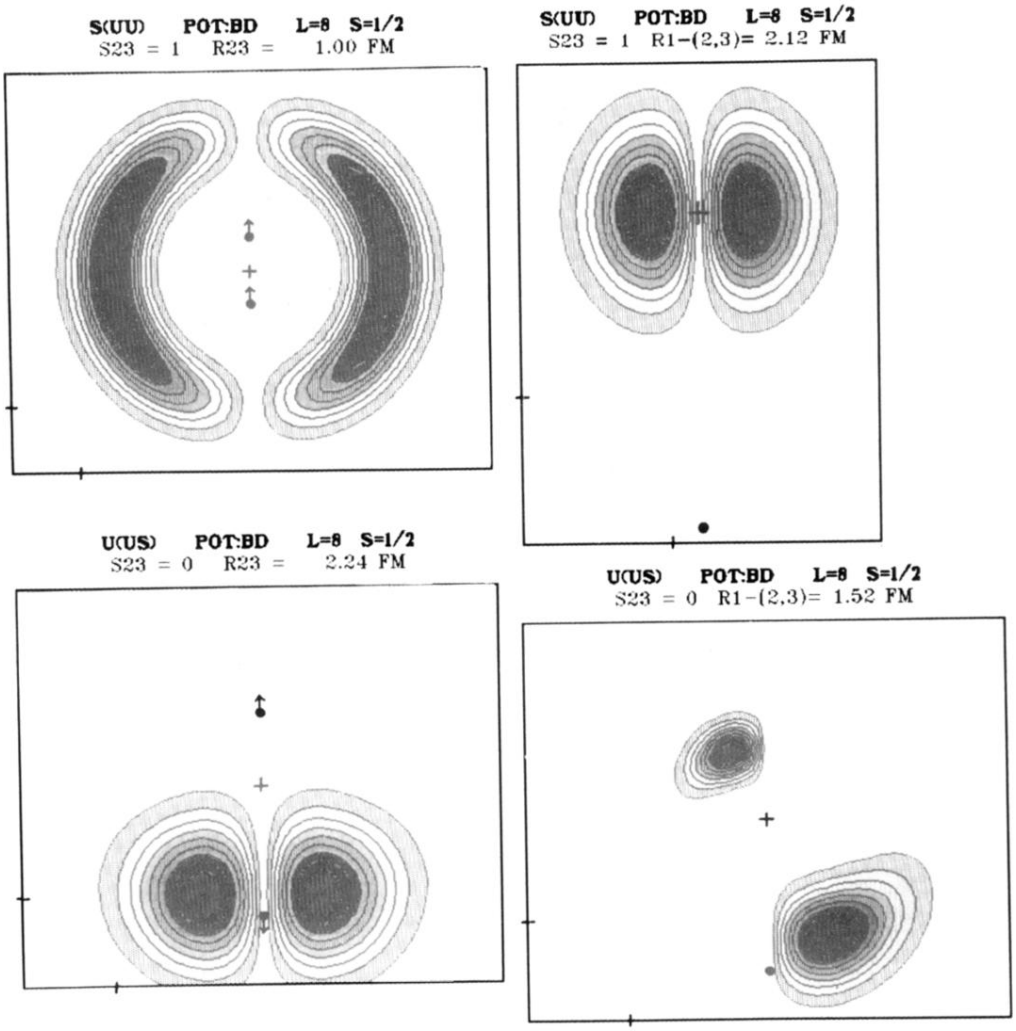

FIG. 6. Three-body densities for the Σ system *suu* in an orbital $L = 8$ excited state. Same comments as in Fig. 3.

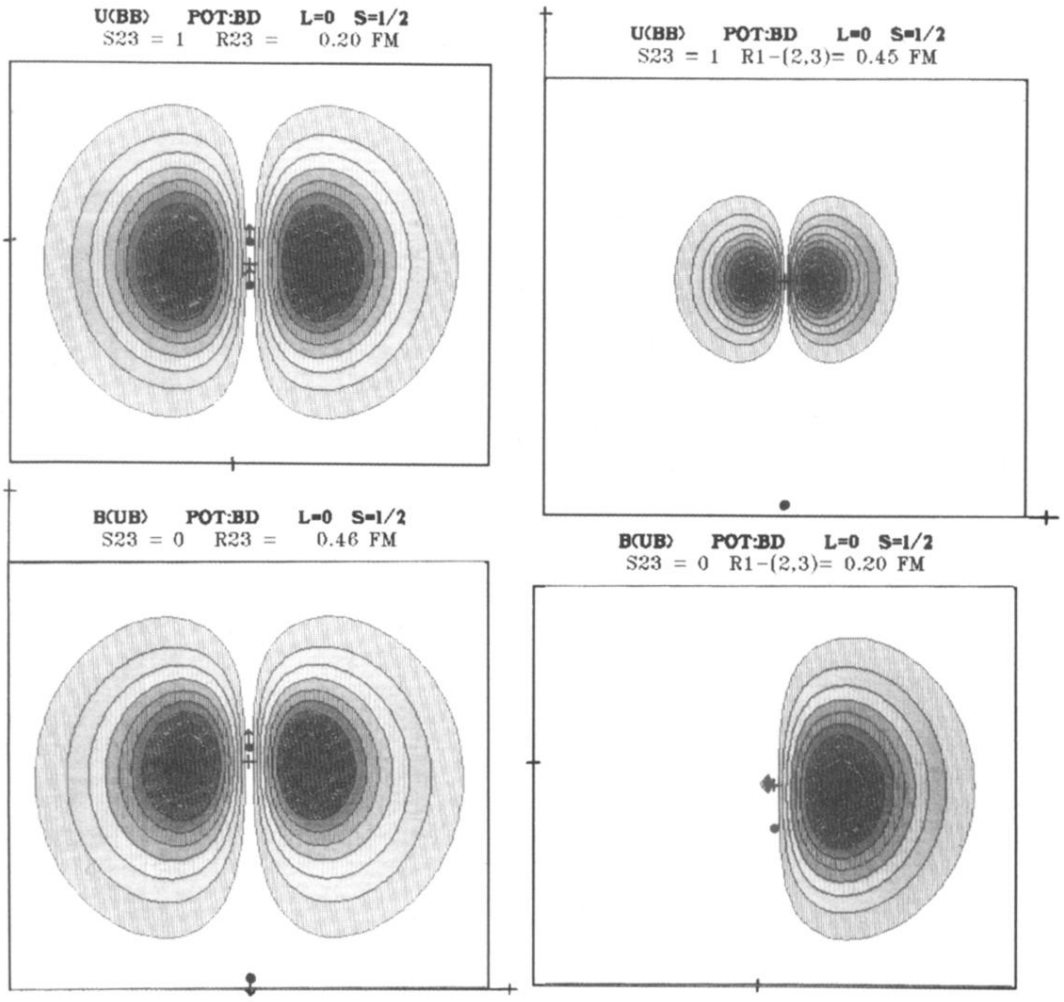

FIG. 7. Three-body densities for the *ubb* in its ground state. Same comments as in Fig. 3.

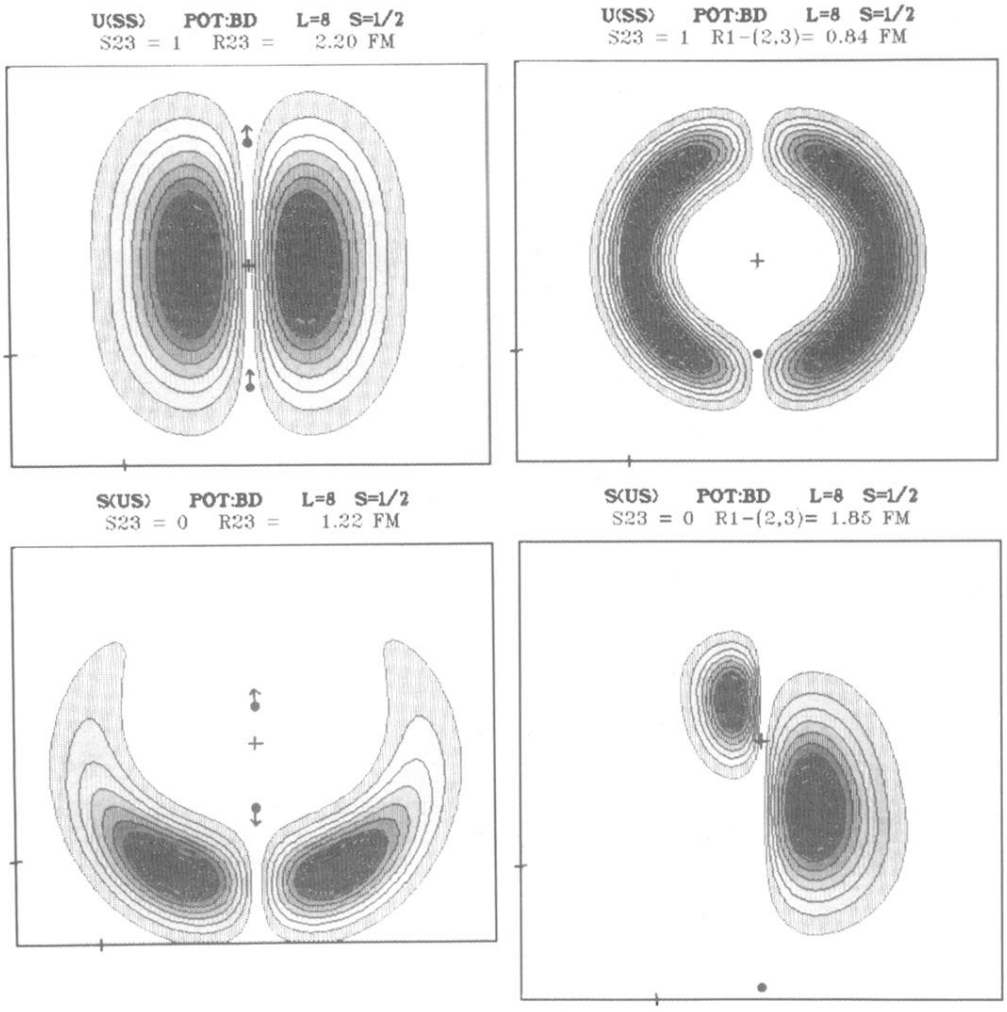

FIG. 8. Three-body densities for the Ξ system *uss* in an orbital $L=8$ excited state. Same comments as in Fig. 3.